Discover Oncology

Research

Activated platelets stimulate effector CD8+ T cells to enhance HNSCC immunotherapy efficacy

Zhennan Yuan[2] · Lunhua Guo[2] · Yuheng Pang[2] · Wenjing Wang[3] · Yuefeng Shang[2] · Chufei Xie[3] · Cheng Qian[2] · Ji Sun[2] · Xiaohong Wu[1]

Received: 29 November 2024 / Accepted: 6 May 2025
Published online: 14 May 2025

Abstract

Programmed Death Receptor-1 (PD-1) is an immune checkpoint receptor expressed on the surface of T cells. Monoclonal antibodies targeting PD-1 and its ligand, PD-L1, are among the most widely utilized immune checkpoint inhibitors in cancer immunotherapy, dramatically improving the prognosis of patients with various malignancies. Traditionally, platelets, which are cytoplasmic fragments derived from megakaryocytes, have been primarily recognized for their roles in hemostasis and coagulation. However, recent studies have highlighted the emerging role of platelets in cancer biology and therapy. Platelets can modulate immune cell functions through various mechanisms, including the release of bioactive molecules and direct interactions with immune cells. A deeper understanding of the interplay between platelets and immune responses could pave the way for novel therapeutic strategies in cancer treatment. In our research, in patients with better treatment responses, there are higher levels of mature and activated CD8+ T cells in their PBMCs prior to treatment. Additionally, the activation of platelets is also more pronounced, and the proteins expressed on these platelets may modulate immune cells. After receiving immunotherapy, patients in the responsive (R) group exhibited a higher abundance of activated effector CD8+ T cells, which demonstrated stronger immune response capabilities. Furthermore, the increased levels of activated platelets in the R group may contribute to the regulation of CD8+ effector memory T cells, influencing their quantity and function. Our study suggests that the functional state of CD8+ T cells and the level of activated platelets prior to treatment may serve as predictive indicators for the efficacy of PD-1 inhibitors in head and neck cancer patients. Activated CD8+ effector T cells may contribute to the differences in immunotherapy responses, with activated platelets playing a role in promoting the maturation and activation of CD8+ effector memory T cells.These insights help better understand the interactions between platelets and immune cells, particularly emphasizing the role of CD8+ effector memory T cells in immunotherapy. Additionally, they offer potential strategies for predicting patient responses to PD-1 inhibitor treatment and optimizing the efficacy of immunotherapy.

Zhennan Yuan, Lunhua Guo, and Yuheng Pang contributed equally in this work.

Supplementary Information The online version contains supplementary material available at https://doi.org/10.1007/s12672-025-02596-y.

✉ Cheng Qian, qiancheng@ems.hrbmu.edu.cn; ✉ Ji Sun, drsunji@163.com; ✉ Xiaohong Wu, wuxiaohong@hrbmu.edu.cn; Zhennan Yuan, yuanzhennan123@hrbmu.edu.cn; Lunhua Guo, drguolunhua@163.com; Yuheng Pang, 2021021693@hrbmu.edu.cn; Wenjing Wang, wangwenjing85321@ccmu.edu.cn; Yuefeng Shang, yuefengshang@hrbmu.edu.cn; Chufei Xie, xiechufei1999@123.com | [1]NHC and CAMS Key Laboratory of Molecular Probe and Targeted Theranostics, The Fourth Affiliated Hospital of Harbin Medical University, No. 37 Yiyuan Street, Nangang District, Harbin 150001, Heilongjiang, People's Republic of China. [2]Department of Oncology Surgery, Harbin Medical University Cancer Hospital, Haping RD NO.150, Harbin 150001, Heilongjiang, People's Republic of China. [3]Beijing Institute of Hepatology, Beijing YouAn Hospital, Capital Medical University, Beijing, China.

Keywords HNSCC · PD-1 · CyTOF · Platelet

Abbreviations

HNSCC	Head and neck squamous cell carcinoma
PBMC	Peripheral blood mononuclear cell
CyTOF	Cytometry by time-of-flight
PD-1	Programmed cell death protein 1
PD-L1	Programmed death-ligand 1
ICB	Immune checkpoint blockade
NR	Non-responder
R	Responder
TCEP	Tris(2-carboxyethyl)phosphine
PRP	Platelet-rich plasma
TGF-β	Transforming growth factor beta

1 Introduction

Cancer remains a significant global health challenge. The latest cancer statistics report indicates that nearly 10 million people die from cancer annually, with almost 20 million new cases diagnosed worldwide each year [1]. HNSCC, including oral cancer, pharyngeal cancer, laryngeal cancer, nasopharyngeal cancer, thyroid cancer, and salivary gland cancer [2], account for over 600,000 new cases globally each year. Many HNSCC patients are diagnosed at an advanced stage. Although treatments like radiotherapy, surgery, and chemotherapy can offer some degree of control over HNSCC, most patients suffer from various long-term side effects. The development of new treatment strategies is currently the top priority in HNSCC research [3].

Immunotherapy has emerged as a pivotal approach in cancer treatment, leveraging the body's immune system to identify and target tumors while restoring its natural anti-tumor capabilities. This approach is particularly beneficial in advanced and metastatic cancers [4], where traditional therapies often fall short. Among the various immunotherapeutic strategies, immune checkpoint inhibitors, especially those targeting the PD-1/PD-L1 pathway, have become integral to cancer treatment. However, monotherapy with immune checkpoint blockade (ICB) may take longer to achieve effective clinical responses. Therefore, combining other therapeutic modalities with immunotherapy has become a major focus in both clinical and preclinical research [5].

Platelets, as a crucial component of the blood system, are primarily recognized for their roles in hemostasis and coagulation [6]. Beyond these traditional functions, they are also involved in immune regulation and vascular repair. Within tumor tissues, platelets can protect tumor cells from immune system attacks, facilitate angiogenesis, and promote metastasis. However, recent research has uncovered a more complex interaction between platelets and immune cells, particularly within the context of cancer. Platelets may directly or indirectly activate immune cells, contributing to anti-tumor effects. This emerging understanding is significant for enhancing the efficacy of tumor immunotherapy and for the development of novel therapeutic strategies [7].

Mass cytometry utilizes metal isotope-conjugated antibodies to label proteins on both the surface and within cells, which are then quantified through mass spectrometry [8]. Traditional fluorescence flow cytometry encounters limitations such as fluorescence signal overlap and the need for compensation, which restrict the number of detectable parameters. In contrast, mass cytometry leverages the distinct molecular weights of isotopes, allowing for the simultaneous detection of over 40 parameters. This capability significantly expands the range of proteins that can be analyzed concurrently [9]. Mass cytometry is particularly valuable for in-depth analysis of cell phenotypes, investigating immune cell diversity, and exploring tumor microenvironments. It has substantial potential for assessing responses to immunotherapy and analyzing immune cell heterogeneity.

In our study, we evaluated the impact of PD-1 therapy on peripheral blood mononuclear cells (PBMCs) in patients with HNSCC, focusing on the differences in PBMC composition and function between non-responders (NR) and responders (R) prior to treatment. We also assessed variations in platelet characteristics and explored the relationship between platelets and immune cell maturation. Additionally, we examined the differential responses of PBMCs to PD-1 therapy in the NR and R groups, with particular attention to the role of platelets in this process. Our findings indicate that, before treatment, CD8 T cells in the NR group were predominantly in an initial, less mature state, whereas those in the R group exhibited

a more mature phenotype. Following PD-1 therapy, the function of CD8 T cells significantly improved in the R group, while no notable changes were observed in the NR group. These disparities in immune cell function and phenotype may be associated with varying activation states of platelets. Therefore, monitoring and analyzing PBMCs and platelets in cancer patients prior to PD-1 treatment could be pivotal in predicting treatment efficacy.

Experimental Design and Statistical Rationale: Patients diagnosed with stage IV HNSCC were enrolled in this study, with all participants providing informed consent. Blood samples were collected at two time points: one day before the initiation of PD-1 inhibitor therapy and after completing four cycles of treatment. Peripheral blood mononuclear cells (PBMCs) were isolated using density gradient centrifugation and cryopreserved for subsequent analysis. Platelet-rich plasma (PRP) was also prepared from the blood samples by centrifugation and used for platelet activation assays and protein expression analysis. To assess the molecular phenotype and heterogeneity of immune cells and platelets, CyTOF (Cytometry by Time-Of-Flight) was performed, enabling the simultaneous detection of multiple proteins at the single-cell level. A correlation matrix was generated to evaluate the relationship between platelet activation levels and immune cell function, particularly focusing on the influence of activated platelets on CD8+ effector memory T cell maturation and function. Statistical analyses were performed using t-tests or ANOVA where applicable, with a p-value < 0.05 considered statistically significant, and correlation coefficients (r-values) were calculated to explore the relationships between variables.

2 Materials and methods

2.1 Patients

This study included 23 patients with HNSCC who received immunotherapy at Harbin Medical University Cancer Hospital. These patients, all diagnosed with stage IV disease, were ineligible for surgical intervention at the time of enrollment. The primary treatment goal was to reduce tumor burden sufficiently to enable subsequent surgical procedures. Patients received PD-1 inhibitor therapy, specifically camrelizumab from Hengrui Medicine, administered at a dose of 200 mg via intravenous infusion every 21 days. The patient received two or three cycles of treatment, with blood samples collected the day before treatment and 21 days after the last treatment. Exclusion criteria included a history of severe thrombocytopenia, significant liver dysfunction, previous severe pulmonary diseases, current respiratory complications, or any known allergic reactions to PD-1 inhibitors or their components. In addition to the patient cohort, 10 healthy individuals were recruited as controls. According to the RECIST 1.1 criteria, a tumor shrinkage of ≥30% or complete disappearance is classified as the response group (R). If there is no significant shrinkage (tumor reduction less than 30%) or no notable change in tumor size, it is defined as the non-response group (NR). All participants provided informed consent. Clinical details of the patients are provided in Supplementary Table 1. The study was conducted in accordance with the principles of the Helsinki Declaration and was approved by the Ethics Committee of Harbin Medical University Cancer Hospital.

2.2 Agents

The antibodies used for the detection of proteins in peripheral blood mononuclear cells (PBMCs) and platelets are detailed in Supplementary Tables 2 and 3. Some of these antibodies were acquired as commercially available metal-conjugated antibodies, while others were custom-conjugated using metal-conjugation technology provided by Standard Biotools. Additional reagents and tools utilized in the study included the Maxpar X8 Multi-Metal Labeling Kit, EQ Four Element Calibration Beads, FixI, Fix and Perm solutions, Cell-ID Intercalator-IR, and the 20X barcoding kit, all of which were sourced from Standard Biotools. Dulbecco's Phosphate-Buffered Saline (DPBS) was purchased from Corning, and EDTA anticoagulant tubes were obtained from BD. TCEP was supplied by Thermo Fisher Scientific, cell cryopreservation solution was sourced from Stemcell Technologies, antibody storage solution was acquired from Candor Bioscience, and 3k and 50k molecular weight cutoff filters were obtained from Amicon Ultra.

2.3 Antibody metal labeling

To begin the antibody metal labeling process, 95 µL of L-Buffer was added to the X8-polymer tube and mixed until the polymer was fully dissolved, followed by the addition of 5 µL of a 50 mM lanthanide metal solution. The mixture was then incubated in a 37 °C water bath for 30 min. Meanwhile, 100 µg of the antibody, with a total volume not exceeding 400 µL, was placed into a 50k filter column, and R-Buffer was added to bring the total volume to 400 µL. The filter column was centrifuged at 12,000×*g* at room temperature for 10 min. TCEP was diluted to a final concentration of 4 mM (1:100) in R-Buffer. Next, 200 µL of L-Buffer was added to a 3k filter column, and the metal-polymer mixture was transferred to the 3k filter column, which was then centrifuged at 12,000×*g* at room temperature for 30 min. Afterward, 100 µL of the 4 mM TCEP solution was added to the antibody-containing 50k filter column, mixed thoroughly, and immediately incubated in a 37 °C water bath for 30 min. The waste liquid from the collection tube of the 3k filter column was discarded, and 400 µL of C-Buffer was added to the filter column, which was centrifuged at 12,000×*g* at room temperature for 30 min. Subsequently, 300 µL of C-Buffer was added to the 50k filter column, centrifuged at 12,000×*g* at room temperature for 10 min, followed by a second wash with an additional 400 µL of C-Buffer, and centrifuged again at 12,000×*g* for 10 min. The correct correspondence between each antibody and metal was confirmed, after which 60 µL of C-Buffer was added to the 50k filter cartridge, the liquid was transferred, gently mixed by pipetting, and incubated in a 37 °C water bath for 90 min. Following incubation, 300 µL of W-Buffer was added to the filter cartridge, which was then centrifuged at 12,000×*g* at room temperature for 10 min, the waste liquid was discarded, and the filter cartridge was washed three times with W-Buffer. Finally, 100 µL of antibody storage solution was added to the filter cartridge, which was inverted over a new collection tube and centrifuged at 1000×*g* at room temperature for 2 min to collect the labeled antibody for storage.

2.4 PBMC and platelet-rich plasma preparation

Whole blood collected in EDTA anticoagulant tubes was initially centrifuged at 200×*g* for 15 min to separate the platelet-rich plasma (PRP), which was then collected. The PRP was subjected to a second centrifugation at 800×*g* for 15 min, after which 200 µL of the platelet-rich pellet was retained. For the preparation of peripheral blood mononuclear cells (PBMCs), Ficoll-Paque density gradient centrifugation was employed. Lymphocyte separation solution was added to the Sepmate tube chamber until it covered the divider (15 mL). An equal volume of blood cells mixed with DPBS containing 2% FBS was carefully layered on top of the Sepmate tube. Gradient centrifugation was performed at 1200×*g* for 15 min, with acceleration to speed level 3 and deceleration to speed level 1. The white PBMC layer was aspirated, resuspended in DPBS containing 2% FBS, and centrifuged at 400×*g* for 8 min. Red blood cells were lysed by adding 3 mL of red blood cell lysis solution, mixing, and allowing it to react for 5 min, followed by the addition of 3 mL of DPBS containing 2% FBS. This mixture was then centrifuged at 500×*g* for 5 min. To label live cells, 500 µL of 0.01% cisplatin was added, mixed, and incubated at room temperature for 2 min. Following this, DPBS containing 5% FBS was added and centrifuged at 500×*g* for 5 min. To fix the cells, 500 µL of 1.6% paraformaldehyde was added, mixed, and incubated for 15 min. Afterward, 1 mL of DPBS containing 5% FBS was added, and the mixture was centrifuged at 500×*g* for 5 min. The supernatant was discarded, and 1 mL of cell storage solution was added to each sample before storing at −80 °C.

2.5 Metal-conjugated antibody labeling of PBMCs and platelets

To prepare PBMCs, mix Barcode Perm with the isolated PBMCs, centrifuge at 800×*g* for 5 min, and repeat this step twice. Next, add 100 µL of Barcode Perm to the 20-Plex Pd Barcoding Sets, mix well, and combine with the PBMC samples according to the experimental grouping plan. Vortex to ensure thorough mixing and incubate at room temperature for 30 min. To terminate the reaction, add 1 mL of DPBS containing 5% FBS, centrifuge at 800×*g* for 5 min, discard the supernatant, and resuspend the cells in 1 mL of DPBS containing 5% FBS. Centrifuge at 800×*g* for 5 min twice, discard the supernatant, and resuspend each sample tube in 100 µL of DPBS containing 5% FBS. Combine all tubes, centrifuge at 800×*g* for 5 min, and add the antibody mix (Supplementary Table 2). Incubate at room temperature for 30 min. After incubation, add 1 mL of DPBS containing 5% FBS, centrifuge at 800×*g* for 5 min, and discard the supernatant. Add 1 mL of FixI fixative, mix thoroughly, and centrifuge at 800×*g* for 5 min, discarding the supernatant. Wash the samples twice with 1 mL of DPBS, then mix with 100 µL of DPBS, vortex, and add 0.1% Ir500 µL. Incubate overnight at 4 °C. Before analysis,

wash the samples three times with pure water. Mix with cell collection buffer containing 10% EQ beads, filter through a 40 µm mesh, and keep on ice until further analysis on the instrument.

For platelet-rich plasma (PRP), mix directly with the antibody mix (Supplementary Table 3). Incubate at room temperature for 30 min, then resuspend in 1 mL of DPBS and centrifuge at 800×*g* for 10 min. Resuspend the pellet in 1 mL of FixI fixative and centrifuge at 800×*g* for 10 min. Wash twice with pure water. Mix with cell collection buffer containing 10% EQ beads, filter through a 40 µm mesh, and keep on ice until further analysis on the instrument.

2.6 CyTOF data analysis

CyTOF 7.0 software was used to process the FCS files obtained from the Helios (Standard Biotools) instrument. Raw files were normalized to produce standardized FCS files, and individual PBMC sample files were separated using the debarcode tool. The processed data were then uploaded to Cytobank (https://www.cytobank.org) for further data cleaning. Signals from EQ beads were removed, and cell debris and aggregates were excluded based on event length. Dead cells were identified and removed using platinum labeling signals, and CD45-positive immune cells were selected for analysis. The cleaned FCS files were subsequently exported. For platelet data, the FCS files were also uploaded to Cytobank, where CD41a-positive platelets were identified based on surface protein expression. Further analysis was conducted using R (https://bioconductor.org/packages/cytofkit/). Data visualization and interpretation were enhanced through the application of Phenograph clustering and t-SNE (t-distributed Stochastic Neighbor Embedding) for dimensionality reduction. Additional analyses of cluster subpopulation content, protein expression statistics, and correlation analysis were performed using Sangbox (http://www.sangerbox.com/login.html) and GraphPad Prism.

2.7 Correlation analysis

The Pearson correlation coefficient, denoted as r, measures the strength and direction of the linear relationship between two continuous variables. It ranges from −1 to 1, where −1 indicates a perfect negative correlation, 0 indicates no correlation, and 1 indicates a perfect positive correlation. The magnitude of r indicates the strength of the correlation, with values closer to -1 or 1 signifying stronger correlations.

3 Results

3.1 Immune cell composition in PBMCs and its association with PD-1 therapy response in HNSCC

PBMCs from healthy individuals, as well as from patients before and after PD-1 treatment, were collected and analyzed using mass cytometry, focusing on the expression of specific surface proteins on immune cells. The initial analysis identified a total of 13 distinct cell subpopulations (Fig. 1A). Protein expression patterns are shown in the t-SNE heatmaps (Fig. 1B), more detailed protein expression patterns are shown in Supplementary materials (Supplementary Fig. 1A). Based on the protein expression patterns of each subpopulation, immune cells were defined and their proportions were statistically analyzed (Supplementary Fig. 1B). The highest proportion was activated CD4+ helper T cells, which accounted for about 20%, while the lowest proportion was terminally differentiated CD4+ T cells, which accounted for about 2% (Fig. 1C, D). Significant variations in the proportion of cell subpopulations were noted across different groups (Fig. 1E). Comparing the immune cell proportions in PBMCs from healthy individuals and patients before and after treatment, we found that, compared with healthy individuals, the proportion of terminally differentiated CD4+ T cells and myeloid dendritic cells was significantly increased in patient samples, while CD4+ memory helper T cells, regulatory T cells, and memory B cells were significantly reduced. After PD-1 inhibitor treatment, the proportions of CD8+ effector T cells, neutrophils, and memory B cells were significantly increased, while terminally differentiated CD8+ T cells and NKT cells were significantly reduced. In summary, there were significant differences in the composition of PBMCs between healthy individuals and patients before and after treatment. These differences may be related to tumor progression and treatment response. To better analyze and utilize these differences, we grouped the patients based on their treatment responses and conducted further analysis.

Fig. 1 Analysis of peripheral blood mononuclear cells (PBMC) differences in healthy donors and patients before and after treatment. ▶ **A** Clustering analysis of PBMCs from healthy controls, pre-treatment, and post-treatment patients based on cell surface proteins using CyTOF, generating a t-SNE plot (*HD* healthy donors, *PRE* pre-treatment patients, *POST* post-treatment patients). **B** Protein expression levels are displayed using a t-SNE heatmap. Color bars range from *red* to *blue*, with *red* indicating high expression. **C** Expression of PBMC subpopulation markers is shown in a heatmap format. Color bars range from *red* to *white*, with *red* indicating high expression. **D** The proportions of PBMC subpopulations are displayed in a bar chart, with cells defined based on the protein expression levels of each subpopulation. **E** Proportions of PBMC subpopulations in each sample are shown in stacked bar graphs

3.2 Immune cell subpopulations and their correlation with PD-1 therapy response in HNSCC

Comparative analysis of PBMC samples from healthy individuals and pre-treatment samples from PD-1 therapy patients clustered into 12 distinct cell subpopulations based on protein expression levels (Fig. 2A). The cells were categorized according to their protein expression profiles, with the highest proportion being monocytes and the lowest proportion being myeloid dendritic cells (DCs). CD8+ T cells, a key player in immune therapy, are one of the primary cell subpopulations where therapeutic effects are exerted. In our analysis, two subpopulations, possibly corresponding to CD8+ T cells, were identified. Comparing their protein expression profiles revealed that subpopulation 1 expressed higher levels of proteins such as CD57 and CD27, suggesting a more mature and functionally active state. In contrast, subpopulation 12 expressed PD-1, indicating a potentially immunosuppressive or exhausted state due to prolonged stimulation. When comparing the abundance of these cell subpopulations, we observed that, unlike our previous comparison between healthy individuals and pre-treatment patient samples, the abundance of subpopulation 12 was significantly higher in the non-responder (NR) group compared to the responder (R) group. Conversely, subpopulation 1 was more prevalent in the R group (Fig. 2B, C). Additionally, we found differences in the functional activity of cell subpopulation 1 between pre- and post-treatment samples (Fig. 2D). Subpopulation 1 in the R group, which exhibited higher expression levels of functional proteins such as CD28, CD127, ICOS, CD27, and CD197 compared to the NR group, is likely to represent CD8+ effector memory T cells. Moreover, PD-1 expression was notably higher in subpopulation 1 of the NR group (Fig. 2E). In summary, patients who responded well to PD-1 inhibition therapy had a higher abundance of activated CD8+ T cells in their pre-treatment blood, and these cells also exhibited stronger functional activity.

3.3 Platelet activation and its potential role in predicting response to PD-1 inhibition in HNSCC

Platelets play a complex role in immune responses, interacting with various immune cells to modulate immune functions [10]. To explore the role of platelets in cancer immunotherapy and their impact on therapeutic outcomes, we isolated platelets from patient plasma and examined their functionality and key activation markers. Mass cytometry was used to analyze the platelet-rich plasma (PRP) from healthy individuals and patients prior to PD-1 inhibitor treatment. Based on platelet function and the expression of activation-related proteins, the samples were analyzed and clustered into 13 platelet subpopulations (Fig. 3A). The protein expression patterns are shown in the t-SNE heatmaps (Fig. 3B), and more detailed protein expression patterns can be found in the supplementary materials (Supplementary Fig. 2A). Clustering analysis revealed that several platelet activation markers, such as CD62P, CD63, and CD29, were highly expressed in platelet subpopulations 3, 6, and 8, indicating that these subpopulations likely represent activated platelets (Fig. 3B). Compared to other platelet subpopulations, subpopulation 6 was found to simultaneously express high levels of CD183, CD184, and CD185, which may be involved in regulating the chemotaxis of platelets in immune responses. Additionally, CD51/61 enables faster aggregation, CD107A confers enhanced functionality, and CD31 promotes closer interactions between this subpopulation and immune cells. The distribution of platelet subpopulations differs significantly between the groups (Supplementary Fig. 2B). Upon comparing the distribution of these activated platelet subpopulations across different groups, we found that subpopulations 6 and 8 were more abundant in healthy individuals and samples from responders (R) to therapy. To determine whether platelet activation is associated with the functional state of T cells, we compared the protein expression levels in these platelet subpopulations across different patient groups. Proteins involved in T cell function, including TLR4, TLR2, CD62P, and CD107A, were upregulated in the responder (R) group (Fig. 3C, F). Therefore, we propose that activated platelets may influence immune cells in the PBMCs, particularly T cells. In abundance correlation analysis, we observed a positive correlation between platelet subpopulations 6 and 8 and T cell subpopulation 1 in the R group (Fig. 3G,

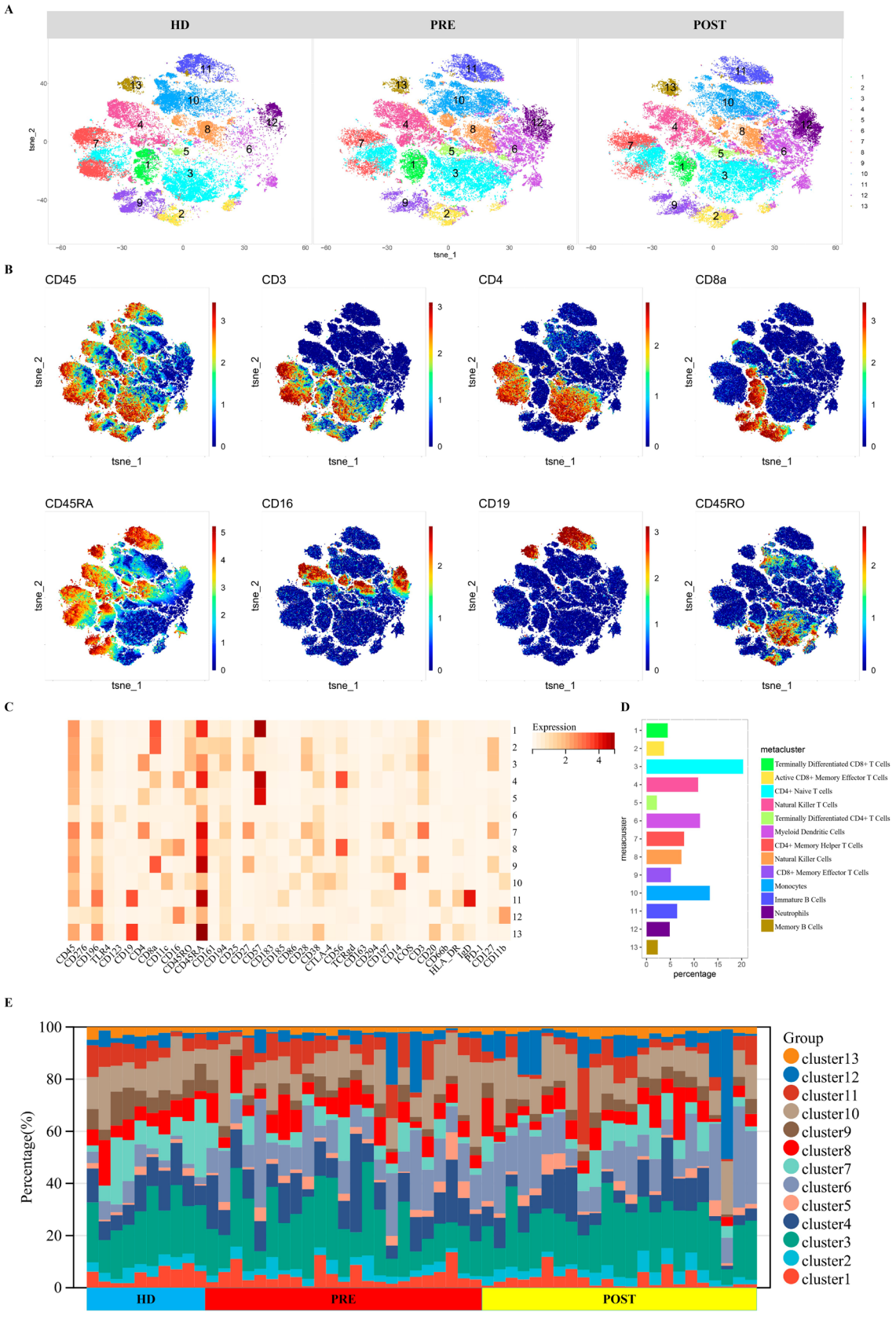
A
HD
PRE
POST
tsne_1
tsne_2
B
CD45
CD3
CD4
CD8a
CD45RA
CD16
CD19
CD45RO
C
Expression
D
metacluster
Terminally Differentiated CD8+ T Cells
Active CD8+ Memory Effector T Cells
CD4+ Naive T cells
Natural Killer T Cells
Terminally Differentiated CD4+ T Cells
Myeloid Dendritic Cells
CD4+ Memory Helper T Cells
Natural Killer Cells
CD8+ Memory Effector T Cells
Monocytes
Immature B Cells
Neutrophils
Memory B Cells
percentage
E
Percentage(%)
Group
cluster13
cluster12
cluster11
cluster10
cluster9
cluster8
cluster7
cluster6
cluster5
cluster4
cluster3
cluster2
cluster1
HD
PRE
POST

Fig. 2 Analysis of PBMC subpopulations before PD-1 treatment in NR and R groups. **A** Clustering analysis of PBMCs from each group based on cell surface proteins using CyTOF, generating a t-SNE plot (*HD* healthy donors, *PRE_NR* pre-treatment samples from the Non-response group, *PRE_R* pre-treatment samples from the Response group) **B** Expression of PBMC subpopulation markers is shown in a heatmap format. Color bars range from *yellow* to *violet*, with *yellow* indicating high expression. **C** Proportions of PBMC subpopulations are displayed in a donut chart. **D** Box plot comparing the proportions of PBMC subpopulations among the groups. **E** Comparison of expression levels of CD28, CD127, ICOS, CD27, CCR7, and PD-1 in PBMC subpopulation 1 across groups. ($0.01 < p \leq 0.05$: significant difference; $0.001 < p \leq 0.01$: strong significant difference; $p \leq 0.001$: extremely significant difference; $p \leq 0.0001$: very extremely significant difference)

H). In contrast, no such correlation was observed in the NR group (Supplementary Fig. 2C). This suggests that the activation state of specific platelet subpopulations before immunotherapy may potentially facilitate the maturation of CD8+ T cells. Thus, assessing platelet activation levels and the activation state of CD8+ T cells could serve as a useful reference for predicting the response to immunotherapy in HNSCC.

3.4 Differential response of activated CD8 + effector memory T Cells following immunotherapy

To evaluate the impact of immunotherapy on patients' PBMCs and identify the main functional cells involved in immunotherapy, we analyzed PBMCs from patients before and after treatment, based on protein expression profiles. Clustering analysis identified 11 immune cell subpopulations (Fig. 4A). Based on their protein expression profiles, we defined and quantified the subpopulations. The most abundant subpopulation was CD4+ naïve T cells, while NK cells accounted for the lowest proportion. Among the CD8+ T cells, we focused on two subpopulations: CD8+ effector memory T cells and activated CD8+ effector memory T cells (Fig. 4B, C). Comparison of immune cell abundances between groups revealed that in the R group, immunotherapy led to a decrease in the abundance of CD4+ memory helper T cells. In the NR group, there was no significant difference in the abundance of this cell population before and after treatment, but a marked decrease in initial CD4+ T cells was observed. In the R group, the abundance of activated CD8+ effector memory T cells increased after treatment, significantly higher than both pre-treatment levels and those in the NR group. In contrast, the abundance of another CD8+ effector T cell subpopulation significantly decreased in the NR group post-treatment, which may indicate that this subpopulation of CD8+ effector T cells failed to recover effectively after immunotherapy, suggesting insufficient immune reserve and weaker response capability to immunotherapy (Fig. 4D). We performed paired comparisons of Subpopulation 4 (activated CD8+ effector memory T cells) before and after treatment. In the R group, the abundance of this subpopulation generally increased, with statistically significant differences observed, while in the NR group, the changes in abundance were highly variable across individual samples, with no significant differences detected (Supplementary Fig. 3A). Subpopulation 4 in the R group exhibited higher levels of T cell function-related proteins, including CD27, CD25, CD57, CD28, CD127, and ICOS, compared to the NR group, indicating a stronger response capability (Fig. 4E). In contrast, the NR group showed no significant changes in the proportion of Subpopulation 4 or in the expression levels of T cell function proteins before and after treatment (Supplementary Fig. 3B). These findings suggest that immunotherapy significantly increased the abundance of activated CD8+ effector memory T cells in the R group, reflecting a stronger immune response triggered by the treatment. In contrast, the NR group showed no significant changes in immune cell subpopulations, and the recovery of CD8+ effector T cells was insufficient, which may contribute to a weaker response to immunotherapy. Additionally, the increase in activated CD8+ effector memory T cells in the R group was associated with elevated expression levels of T cell function-related proteins, further supporting its stronger immune response capability.

3.5 Platelet subpopulation activation may affect PD-1 therapy efficacy through CD8 T cell function

To explore the potential reasons behind the different immune cell functional states in patients, we separated platelets from both responder (R) and non-responder (NR) groups before and after treatment. Based on platelet function and the expression of activation-related proteins, the samples were analyzed and clustered into 10 platelet subpopulations (Fig. 5A). The protein expression patterns are shown in the t-SNE heatmaps (Fig. 5B), and more detailed protein expression patterns can be found in the supplementary materials (Supplementary Fig. 4A). Clustering analysis revealed that several platelet activation markers, such as CD62P, CD63, and CD29, were highly expressed in platelet subpopulations 6, 7, and 8, indicating that these subpopulations likely represent activated platelets (Fig. 5B and Supplementary Fig. 4B). Analysis of platelet subpopulations revealed that in the NR group, subpopulations 1 and 4 significantly increased after treatment. Platelet subpopulations 6 and 8 showed a significant increase in the R group post-treatment (Fig. 5C). To investigate the roles of these activated and non-activated platelets in the immune response, we compared the expression of several


A
HD
PRE_NR
PRE_R
tsne_1
tsne_2
B
Expression
C
1 Active CD8+ Memory Effector T Cells
2 Immature B Cells
3 Natural Killer T Cells
4 Terminally Differentiated CD4+ T Cells
5 Natural Killer Cells
6 Neutrophils
7 Monocytes
8 Unidentified cells
9 Myeloid Dendritic Cells
10 CD4+ Memory Helper T Cells
11 CD4+ Naive T cells
12 CD8+ Memory Effector T Cells
5.54%
8.28%
6.77%
8.16%
3.58%
5.90%
14.73%
9.41%
2.61%
15.33%
10.44%
9.26%
D
Percentage (%)
File_ID
HD
PRE_NR
PRE_R
cluster1
cluster2
cluster3
cluster4
cluster5
cluster6
cluster7
cluster8
cluster9
cluster10
cluster11
cluster12
E
Expression
Group
HD
PRE_NR
PRE_R
CD196
CD194
CD27
CD28
CD197
ICOS
CD279
CD127

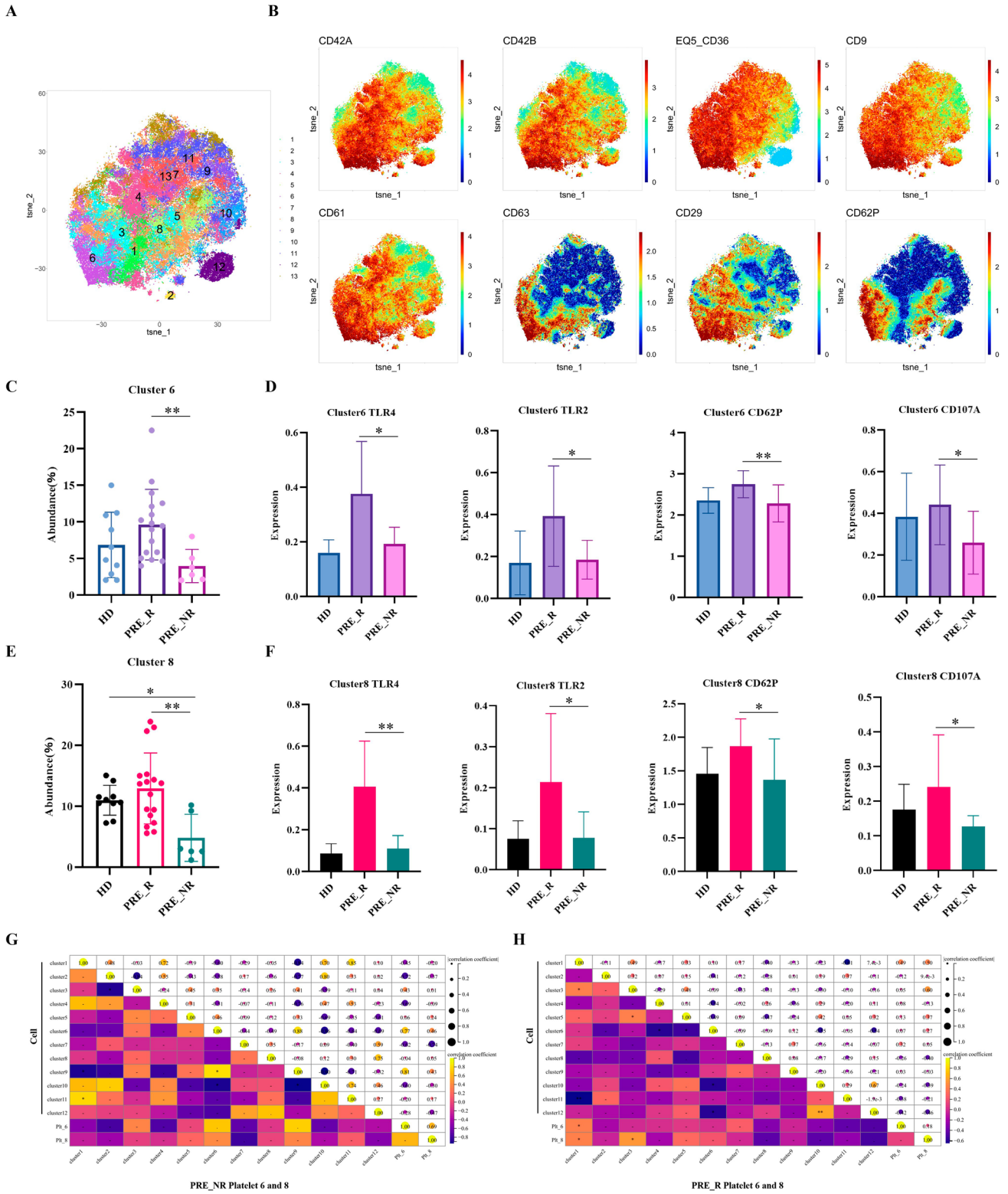

Fig. 3 Analysis of platelet subpopulations before PD-1 treatment in NR and R groups. **A** Clustering analysis of platelets based on cell surface proteins using CyTOF, generating a t-SNE plot (*HD* healthy donors, *PRE_NR* pre-treatment samples from the Non-response group, *PRE_R* pre-treatment samples from the Response group). **B** Protein expression levels are displayed using a t-SNE heatmap. Color bars range from *red* to *blue*, with *red* indicating high expression. **C** Box plot comparing the proportions of platelet subpopulation 6 among the groups. **D** Bar graph comparing the expression levels of TLR4, TLR2, CD62P, and CD107A proteins in platelet subpopulation 6. **E** Proportions of platelet subpopulation 8 in each group. **F** Expression levels of TLR4, TLR2, CD62P, and CD107A proteins in platelet subpopulation 8. **G**, **H** Correlation analysis between the proportions of PBMC subpopulation with platelet subpopulation 6 and 8 in patients (*$0.01 < p \leq 0.05$: significant difference; **$0.001 < p \leq 0.01$: strong significant difference)

Fig. 4 CD8 T cell subpopulations may influence PD-1 treatment efficacy. **A** Clustering analysis of PBMCs from response and non-response groups before and after treatment using CyTOF, generating a t-SNE plot (*NR* non-response, *R* response group, *PRE* pre-treatment, *POST* post-treatment). **B** PBMC subpopulation marker expressions are shown as a heatmap. Color bars range from *purple* to *white*, with *purple* indicating high expression. **C** Proportions of PBMC subpopulations are displayed in a Donut chart. **D** Box plot comparing the proportion of PBMC subpopulation before and after treatment. **E** Comparison of CD27, CD57, CD127, CD25, CD28, and ICOS expression levels in PBMC subpopulation 4 in R group. ($0.01 < p \leq 0.05$: significant difference; $0.001 < p \leq 0.01$: strong significant difference; $p \leq 0.001$: extremely significant difference)

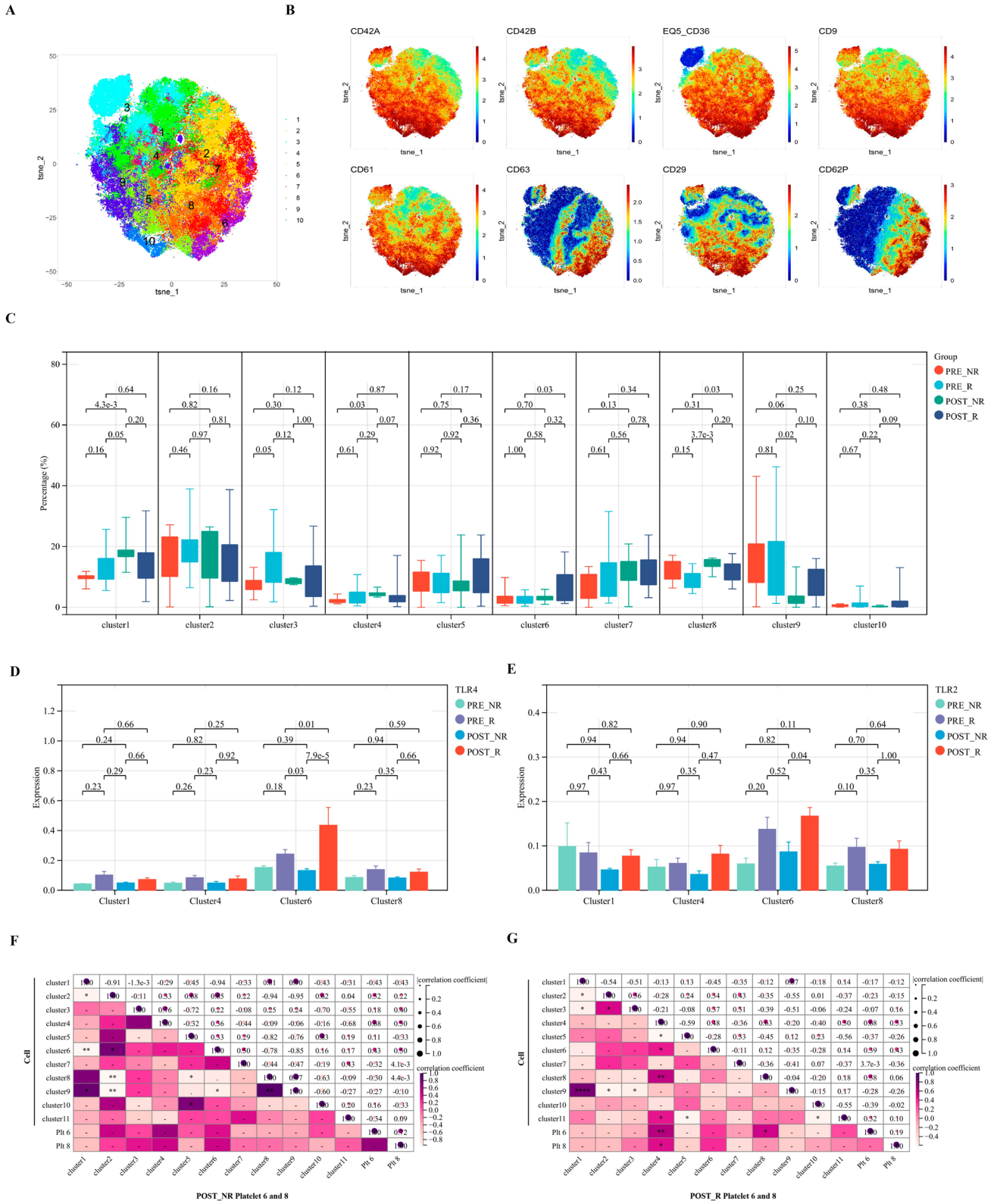

Fig. 5 Platelet subpopulation activation may affect PD-1 treatment efficacy by influencing CD8 T cell function. **A** Clustering analysis of platelets from response and non-response groups before and after treatment using CyTOF, generating a t-SNE plot (*NR* non-response, *R* response group, *PRE* pre-treatment, *POST* post-treatment). **B** Expression of platelet markers is shown as a t-SNE heatmap. Color bars range from *red* to *blue*, with *red* indicating high expression. **C** Box plot comparing the proportion of PBMC subpopulation before and after treatment. **D**, **E** Bar graph comparing the expression levels of TLR4, TLR2 proteins in platelet subpopulation 1, 4, 6, 8. **F**, **G** Correlation analysis between the proportions of PBMC subpopulation with platelet subpopulation 6 and 8 in patients (*$0.01 < p \leq 0.05$: significant difference; **$0.001 < p \leq 0.01$: strong significant difference; $p \leq 0.001$: extremely significant difference; ****$p \leq 0.0001$: very extremely significant difference)

platelet-associated immune markers. Compared to other subpopulations, TLR4, TLR2, CD40L, CD107A, CD62P, and CD61 were highly expressed in platelet subpopulations 6 and 8 (Supplementary Fig. 4C–F). We also found that in the R group, TLR4 and TLR2 expression in platelet subpopulation 6 significantly increased post-treatment, whereas in the NR group, although there was an upward trend, the difference was not significant (Fig. 5D, E). To explore the relationship between platelet activation and PBMC components, we conducted a correlation analysis between immune cells and activated platelets. The analysis revealed a positive correlation between the abundance of activated platelets in the R group and the proportion of activated CD8+ effector memory T cells, while no significant correlation was detected in the NR group (Fig. 5F, G). These findings suggest that the expression of immune markers on activated platelets may have a potential impact on immune cells, particularly the quantity and function of CD8+ effector memory T cells. The expression of Toll-like receptors on platelets may reflect the regulatory capacity of the immune response, and their interaction with immune cells could provide new insights for predicting and improving the efficacy of immunotherapy.

4 Discussion

Programmed cell death protein-1 (PD-1) is a surface receptor on T cells that interacts with its ligands, PD-L1 or PD-L2, to inhibit T cell activity [11]. This mechanism, under normal conditions, effectively prevents the immune system from attacking healthy tissues. However, in the context of tumor development, tumors exploit this pathway to evade immune system eradication. In immune checkpoint blockade (ICB) therapy, monitoring peripheral blood mononuclear cells is crucial for revealing the trajectory and functional evolution of T cells within the tumor [12]. By tracking different cell subsets, especially T cells, we can follow the dynamic changes of tumor-reactive T cell clones in both peripheral blood and the tumor microenvironment. This process not only helps in understanding the mechanisms of immune response but also provides key insights for predicting immune therapy outcomes and optimizing treatment strategies [13]. CD8+ T cells, as primary effector T cells, play a crucial role in immune responses, and the expression of PD-1 on activated CD8+ T cells is a key mechanism by which tumors achieve immune escape. Numerous studies have highlighted the significant relationship between CD8+ T cells and immune therapies across various cancers [14–16]. Recent advancements in immune checkpoint inhibitors have been notable, with over ten PD-1 monoclonal antibodies now approved for clinical [17]. Despite the introduction of these novel therapeutic strategies and some degree of success in cancer immunotherapy, challenges such as low response rates and acquired resistance persist [18]. Thus, exploring the role of CD8+ T cells in PD-1 therapy for cancer and understanding the reasons behind incomplete responses in non-responding patients remain critical research priorities.

Platelets, originating from megakaryocytes in the bone marrow, primarily function in hemostasis and coagulation. Recently, their role in immune modulation has gained considerable attention. The complex interactions between platelets and immune cells can influence disease progression and treatment, including innate immune diseases and cancer immunotherapy [19]. Platelets exert intricate regulatory effects on T cells; for example, they secrete transforming growth factor-beta (TGF-β), which can contribute to tumor evasion of immune system recognition, while also releasing interleukins that may promote T cell activation and proliferation. Additionally, PD-L1 on the platelet surface binds to PD-1 on T cells, inhibiting T cell activation and effector functions and inducing T cell exhaustion [20]. Platelets also express CD40L, which binds to CD40 on T cells, thereby promoting T cell proliferation and effector functions [21]. Within tumor tissues, extensive research suggests that platelets may facilitate tumor progression. However, the lack of specificity in targeting tumor-associated platelets and the high risk of systemic complications from anti-platelet therapies highlight the need for targeted interventions that focus on the specific mechanisms of different platelet subpopulations [22]. Furthermore, platelets are an important component in liquid biopsy studies. Variations in platelet RNA and protein profiles can impart functional changes, making this non-invasive detection approach a promising avenue for early cancer detection, prognosis assessment, and personalized treatment [23].

With the rapid advancements in proteomics and flow cytometry techniques, the analysis of cellular subpopulations has become a crucial area of focus. This refined approach allows for precise heterogeneity analyses and cellular mapping, enabling more accurate tracing of molecular-level scientific issues and enhancing our understanding of cellular functional changes. Consequently, it facilitates the development of more targeted intervention strategies. In this study, we employed CyTOF analysis to investigate protein changes in PBMCs and platelets from cancer patients undergoing PD-1 therapy. Our aim was to explore how immune cell and platelet heterogeneity impacts treatment response. We observed notable differences in CD8+ T cell subpopulations between non-responders (NR) and responders (R) prior to treatment. Specifically, the R group exhibited a significant increase in mature CD8+ T cells, whereas the NR group showed a notable

rise in naive CD8+ T cells. We further examined the functionality of mature CD8+ T cells. In the R group, the expression levels of CD28, CD127, ICOS, CD27, and CD197 were significantly higher compared to the NR group. These proteins are crucial for T cell activation, proliferation, and effector functions. Specifically, CD28 is a co-stimulatory molecule essential for T cell effector responses [24]. CD127, the alpha chain of the IL-7 receptor, supports T cell survival and proliferation [25]. ICOS, another co-stimulatory molecule, enhances the retention of CD8+ T cells in tissues through PI3K signaling [26]. CD27, a member of the TNF receptor family, is involved in forming memory T cells and maintaining long-term immune memory [27]. CD197, a chemokine receptor, facilitates the localization and homing of T cells to lymph nodes [28]. Additionally, we observed a significant reduction in PD-1 expression in the R group compared to the NR group. PD-1 is an inhibitory receptor that suppresses T cell activation through interaction with its ligands. Blocking PD-1 can restore T cell anti-tumor activity and is a widely utilized strategy in cancer immunotherapy [29].

To investigate the causes of differences in CD8+ T cell subpopulations, we assessed the expression levels of surface proteins on patient platelets. We observed that platelet activation markers, including CD63, CD62P, and CD29, were significantly higher in the R group compared to the NR group, reflecting greater platelet activation [30, 31]. Additionally, several proteins mediating T cell function, such as TLR4, TLR2, CD62P, and CD107A, were found to be highly expressed. The activation of TLR4 primarily enhances antigen presentation, indirectly influencing T cell activation and function by promoting anti-tumor T cell immunity through immune stimulation and macrophage activation [32, 33]. TLR2 plays a critical role in both innate and adaptive immunity; its activation leads to the release of various inflammatory mediators from platelets, including cytokines and chemokines, which further activate immune cell functions [34, 35]. Platelet CD62P activation may facilitate the recruitment and localization of CD8+ T cells, modulating their functions and enhancing anti-tumor immune responses [36]. CD107A, located on the α-granules and lysosomal granules of platelets, is associated with platelet activation. Platelets participate in immune modulation through the release of microparticles or exosomes, with CD107A involved in the formation and release of these vesicles [37].

To explore the reasons behind different responses to PD-1 therapy, we analyzed protein changes in PBMCs and platelets from the NR and R groups before and after PD-1 treatment. We investigated the relationship between immune cells, platelets, and treatment response. Our analysis revealed a significant increase in the proportion of mature CD8+ T cells in the R group, while no significant changes were observed in the NR group. Functional analysis of the CD8+ T cell subpopulation in the R group showed significantly higher expression levels of CD27, CD25, CD57, CD28, CD127, and ICOS compared to the NR group. CD25-positive CD8+ T cells, which rapidly proliferate and exert potent cytotoxic effects with IL-2 support, play a crucial role in anti-tumor and anti-infection immunity [38, 39]. CD57-positive CD8+ T cells, a distinct subset typically associated with terminal differentiation, reduced proliferative capacity, and strong cytotoxic functions, are likely to represent mature, activated CD8+ effector memory T cells. Analyzing platelet surface proteins revealed that, in the NR group, the two platelet subpopulations that increased were non-activated. In contrast, activated platelet subpopulations in the R group showed a marked increase post-treatment, and the abundance of these activated platelets positively correlated with the quantity of activated CD8+ effector memory T after treatment.

Based on these findings, we hypothesize that the abundance of CD8+ effector memory T cells play a central role in immunotherapy, particularly in predicting therapeutic efficacy. The activation of these T cells is crucial for the effectiveness of immune treatments, and activated platelets may contribute significantly to this process. Toll-like receptors (TLRs) on platelets could play a key role in this interaction, influencing the activation of CD8+ T cells and thereby impacting the overall immune response. Understanding the relationship between platelet activation and T-cell functionality could offer valuable insights into predicting and improving the outcomes of immunotherapy.

This study has certain limitations. The relatively short treatment period, designed to prepare patients for surgery following tumor downstaging, may restrict the ability to comprehensively evaluate the long-term immune responses associated with patient outcomes. As a result, this timeframe may introduce potential biases or limitations in interpreting the findings and drawing broader conclusions. Future studies with extended treatment durations could offer further insights into the dynamic changes in immune responses and their correlation with clinical outcomes.

Acknowledgements Not applicable.

Author contributions X. W. and J. S.designed the project, and revised the manuscript. Z.Y. wrote the original draft. Z.Y., L. G. and Y. P. performed the related CyTOF experiments and analyzed the results. S. Y., C. X., helped with plasma and PBMC preparation. W. W. and C.Q helped design and adjust the steps of the experiment. All authors reviewed the manuscript.

Funding This work was supported by grants from National Natural Science Foundation of China (82173184 to C. Qian), Heilongjiang Provincial Natural Science Foundation (PL2024H185 to Z. Yuan), Haiyan Scientific Research Funding from cancer hospital of harbin medical university

(JJZD2024-32 to Z. Yuan) and Excellent youth project of the Fourth Affiliated Hospital of Harbin Medical University(HYDSYYXQN2023002 to X. Wu).

Data availability The experiment data used to support the findings of this study are available from the corresponding authors upon request.

Declarations

Ethics approval and consent to participate The study was conducted in accordance with the principles of the Helsinki Declaration and was approved by the Ethics Committee of Harbin Medical University Cancer Hospital.All subjects gave informed consent.

Consent for publication All the authors have read and approved present manuscript.

Competing interests The authors declare no competing interests.

References

1. Bray F, Laversanne M, Sung H, Ferlay J, Siegel RL, Soerjomataram I, Jemal A. Global cancer statistics 2022: GLOBOCAN estimates of incidence and mortality worldwide for 36 cancers in 185 countries. CA Cancer J Clin. 2024;74(3):229–63.
2. Bhat AA, Yousuf P, Wani NA, Rizwan A, Chauhan SS, Siddiqi MA, Bedognetti D, El-Rifai W, Frenneaux MP, Batra SK, Haris M, Macha MA. Tumor microenvironment: an evil nexus promoting aggressive head and neck squamous cell carcinoma and avenue for targeted therapy. Signal Transduct Target Ther. 2021;6(1):12.
3. Johnson DE, Burtness B, Leemans CR, Lui VWY, Bauman JE, Grandis JR. Head and neck squamous cell carcinoma. Nat Rev Dis Primers. 2020;6(1):92.
4. Bhatia A, Burtness B. Treating head and neck cancer in the age of immunotherapy: a 2023 update. Drugs. 2023;83(3):217–48.
5. Mei Z, Huang J, Qiao B, Lam AK. Immune checkpoint pathways in immunotherapy for head and neck squamous cell carcinoma. Int J Oral Sci. 2020;12(1):16.
6. Stoiber D, Assinger A. Platelet-leukocyte interplay in cancer development and progression. Cells. 2020;9(4):855.
7. Morris K, Schnoor B, Papa AL. Platelet cancer cell interplay as a new therapeutic target. Biochim Biophys Acta Rev Cancer. 2022;1877(5):188770.
8. Koladiya A, Davis KL. Advances in clinical mass cytometry. Clin Lab Med. 2023;43(3):507–19.
9. Moldoveanu D, Ramsay L, Lajoie M, Anderson-Trocme L, Lingrand M, Berry D, Perus LJM, Wei Y, Moraes C, Alkallas R, Rajkumar S, Zuo D, Dankner M, Xu EH, Bertos NR, Najafabadi HS, Gravel S, Costantino S, Richer MJ, Lund AW, Del Rincon SV, Spatz A, Miller WH Jr, Jamal R, Lapointe R, Mes-Masson AM, Turcotte S, Petrecca K, Dumitra S, Meguerditchian AN, Richardson K, Tremblay F, Wang B, Chergui M, Guiot MC, Watters K, Stagg J, Quail DF, Mihalcioiu C, Meterissian S, Watson IR. Spatially mapping the immune landscape of melanoma using imaging mass cytometry. Sci Immunol. 2022;7(70):eabi5072.
10. Nicolai L, Pekayvaz K, Massberg S. Platelets: orchestrators of immunity in host defense and beyond. Immunity. 2024;57(5):957–72.
11. Keir ME, Butte MJ, Freeman GJ, Sharpe AH. PD-1 and its ligands in tolerance and immunity. Annu Rev Immunol. 2008;26:677–704.
12. Chen Y, Wang D, Li Y, Qi L, Si W, Bo Y, Chen X, Ye Z, Fan H, Liu B, Liu C, Zhang L, Zhang X, Li Z, Zhu L, Wu A, Zhang Z. Spatiotemporal single-cell analysis decodes cellular dynamics underlying different responses to immunotherapy in colorectal cancer. Cancer Cell. 2024;42(7):1268-1285.e1267.
13. Liu B, Zhang Y, Wang D, Hu X, Zhang Z. Single-cell meta-analyses reveal responses of tumor-reactive CXCL13(+) T cells to immune-checkpoint blockade. Nat Cancer. 2022;3(9):1123–36.
14. Kwon M, An M, Klempner SJ, Lee H, Kim KM, Sa JK, Cho HJ, Hong JY, Lee T, Min YW, Kim TJ, Min BH, Park WY, Kang WK, Kim KT, Kim ST, Lee J. Determinants of response and intrinsic resistance to PD-1 blockade in microsatellite instability-high gastric cancer. Cancer Discov. 2021;11(9):2168–85.
15. Obradovic A, Graves D, Korrer M, Wang Y, Roy S, Naveed A, Xu Y, Luginbuhl A, Curry J, Gibson M, Idrees K, Hurley P, Jiang P, Liu XS, Uppaluri R, Drake CG, Califano A, Kim YJ. Immunostimulatory cancer-associated fibroblast subpopulations can predict immunotherapy response in head and neck cancer. Clin Cancer Res. 2022;28(10):2094–109.
16. Oliveira G, Egloff AM, Afeyan AB, Wolff JO, Zeng Z, Chernock RD, Zhou L, Messier C, Lizotte P, Pfaff KL, Stromhaug K, Penter L, Haddad RI, Hanna GJ, Schoenfeld JD, Goguen LA, Annino DJ, Jo V, Oppelt P, Pipkorn P, Jackson R, Puram SV, Paniello RC, Rich JT, Webb J, Zevallos JP, Mansour M, Fu J, Dunn GP, Rodig SJ, Ley J, Morris LGT, Dunn L, Paweletz CP, Kallogjeri D, Piccirillo JF, Adkins DR, Wu CJ, Uppaluri R. Preexisting tumor-resident T cells with cytotoxic potential associate with response to neoadjuvant anti-PD-1 in head and neck cancer. Sci Immunol. 2023;8(87):eadf4968.

17. Yi M, Zheng X, Niu M, Zhu S, Ge H, Wu K. Combination strategies with PD-1/PD-L1 blockade: current advances and future directions. Mol Cancer. 2022;21(1):28.
18. Pang K, Shi ZD, Wei LY, Dong Y, Ma YY, Wang W, Wang GY, Cao MY, Dong JJ, Chen YA, Zhang P, Hao L, Xu H, Pan D, Chen ZS, Han CH. Research progress of therapeutic effects and drug resistance of immunotherapy based on PD-1/PD-L1 blockade. Drug Resist Updat. 2023;66: 100907.
19. Koupenova M, Livada AC, Morrell CN. Platelet and megakaryocyte roles in innate and adaptive immunity. Circ Res. 2022;130(2):288–308.
20. Hinterleitner C, Strahle J, Malenke E, Hinterleitner M, Henning M, Seehawer M, Bilich T, Heitmann J, Lutz M, Mattern S, Scheuermann S, Horger M, Maurer S, Walz J, Fend F, Handgretinger R, Seitz C, Weigelin B, Singer S, Salih H, Borst O, Kopp HG, Zender L. Platelet PD-L1 reflects collective intratumoral PD-L1 expression and predicts immunotherapy response in non-small cell lung cancer. Nat Commun. 2021;12(1):7005.
21. Repsold L, Joubert AM. Platelet function, role in thrombosis, inflammation, and consequences in chronic myeloproliferative disorders. Cells. 2021;10(11):3034.
22. Li S, Lu Z, Wu S, Chu T, Li B, Qi F, Zhao Y, Nie G. The dynamic role of platelets in cancer progression and their therapeutic implications. Nat Rev Cancer. 2024;24(1):72–87.
23. Roweth HG, Battinelli EM. Lessons to learn from tumor-educated platelets. Blood. 2021;137(23):3174–80.
24. Zhao Y, Caron C, Chan YY, Lee CK, Xu X, Zhang J, Masubuchi T, Wu C, Bui JD, Hui E. cis-B7:CD28 interactions at invaginated synaptic membranes provide CD28 co-stimulation and promote CD8(+) T cell function and anti-tumor immunity. Immunity. 2023;56(6):1187-1203. e1112.
25. Hui Z, Ren Y, Zhang D, Chen Y, Yu W, Cao J, Liu L, Wang T, Xiao S, Zheng L, Pu Y, Wei F, You J, Ren X. PD-1 blockade potentiates neoadjuvant chemotherapy in NSCLC via increasing CD127(+) and KLRG1(+) CD8 T cells. NPJ Precis Oncol. 2023;7(1):48.
26. Peng C, Huggins MA, Wanhainen KM, Knutson TP, Lu H, Georgiev H, Mittelsteadt KL, Jarjour NN, Wang H, Hogquist KA, Campbell DJ, Borges da Silva H, Jameson SC. Engagement of the costimulatory molecule ICOS in tissues promotes establishment of CD8(+) tissue-resident memory T cells. Immunity. 2022;55(1):98-114.e115.
27. Hu B, Yu M, Ma X, Sun J, Liu C, Wang C, Wu S, Fu P, Yang Z, He Y, Zhu Y, Huang C, Yang X, Shi Y, Qiu S, Sun H, Zhu AX, Zhou J, Xu Y, Zhu D, Fan J. IFNalpha potentiates anti-PD-1 efficacy by remodeling glucose metabolism in the hepatocellular carcinoma microenvironment. Cancer Discov. 2022;12(7):1718–41.
28. Choi H, Song H, Jung YW. The roles of CCR7 for the homing of memory CD8+ T cells into their survival niches. Immune Netw. 2020;20(3): e20.
29. Gill AL, Wang PH, Lee J, Hudson WH, Ando S, Araki K, Hu Y, Wieland A, Im S, Gavora A, Medina CB, Freeman GJ, Hashimoto M, Reiner SL, Ahmed R. PD-1 blockade increases the self-renewal of stem-like CD8 T cells to compensate for their accelerated differentiation into effectors. Sci Immunol. 2023;8(86):eadg0539.
30. Dudiki T, Veleeparambil M, Zhevlakova I, Biswas S, Klein EA, Ford P, Podrez EA, Byzova TV. Mechanism of tumor-platelet communications in cancer. Circ Res. 2023;132(11):1447–61.
31. Andrianova IA, Khabirova AI, Ponomareva AA, Peshkova AD, Evtugina NG, Le Minh G, Sibgatullin TB, Weisel JW, Litvinov RI. Chronic immune platelet activation is followed by platelet refractoriness and impaired contractility. Int J Mol Sci. 2022;23(13):7336.
32. Revenstorff J, Ludwig N, Hilger A, Mersmann S, Lehmann M, Grenzheuser JC, Kardell M, Bone J, Kotting NM, Marx NC, Roth J, Vogl T, Rossaint J. Role of S100A8/A9 in platelet-neutrophil complex formation during acute inflammation. Cells. 2022;11(23):3944.
33. Yang D, Tian T, Li X, Zhang B, Qi L, Zhang F, Han M, Wang S, Xiao J, Gou Y, Zhang R, Liu Q, Su S, Liu J, Huang X, Gao Q, Hui L, Tang H, Chen Y, Wang H, Wei B. ZNT1 and Zn 2+ control TLR4 and PD-L1 endocytosis in macrophages to improve chemotherapy efficacy against liver tumor. Hepatology. 2024;80(2):312–29.
34. Lee WS, Kim DS, Kim JH, Heo Y, Yang H, Go EJ, Kim JH, Lee SJ, Ahn BC, Yum JS, Chon HJ, Kim C. Intratumoral immunotherapy using a TLR2/3 agonist, L-pampo, induces robust antitumor immune responses and enhances immune checkpoint blockade. J Immunother Cancer. 2022;10(6):4799.
35. Freen-van Heeren JJ. Toll-like receptor-2/7-mediated T cell activation: an innate potential to augment CD8(+) T cell cytokine production. Scand J Immunol. 2021;93(5):e13019.
36. Shang Y, Sun J, Wu X, Wang Q. Activated platelet membrane nanovesicles recruit neutrophils to exert the antitumor efficiency. Front Chem. 2022;10: 955995.
37. Tynngard N, Alshamari A, Mansson F, Ramstrom S. Variation in activation marker expression within the platelet population - a new parameter for evaluation of platelet flow cytometry data. Platelets. 2022;33(8):1113–8.
38. Wu W, Chia T, Lu J, Li X, Guan J, Li Y, Fu F, Zhou S, Feng Y, Deng J, Zou J, Sun J, Yao Y, Ling X, Wu Z, Zhang Y, Xu J, Wang F, Liang X, Wu M, Liu H, Chen B, He K. IL-2Ralpha-biased agonist enhances antitumor immunity by invigorating tumor-infiltrating CD25(+)CD8(+) T cells. Nat Cancer. 2023;4(9):1309–25.
39. Laporte KM, Hernandez R, Santos Savio A, Malek TR. Robust IL-2-dependent antitumor immunotherapy requires targeting the high-affinity IL-2R on tumor-specific CD8(+) T cells. J Immunother Cancer. 2023;11(6):6611.